Chinese Journal of Natural Medicines

***Tripterygium hypoglaucum* extract ameliorates adjuvant-induced arthritis in mice through the gut microbiota**

Jianghui HU, Jimin NI, Junping ZHENG, Yanlei GUO, Yong YANG, Cheng YE, Xiongjie SUN, Hui XIA, Yanju LIU, Hongtao LIU

Citation: Jianghui HU, Jimin NI, Junping ZHENG, Yanlei GUO, Yong YANG, Cheng YE, Xiongjie SUN, Hui XIA, Yanju LIU, Hongtao LIU, *Tripterygium hypoglaucum* extract ameliorates adjuvant-induced arthritis in mice through the gut microbiota, Chinese Journal of Natural Medicines, 2023, 21(10), 730-744. doi: 10.1016/S1875-5364(23)60466-2.

View online: https://doi.org/10.1016/S1875-5364(23)60466-2

Available online at www.sciencedirect.com
ScienceDirect
Chinese Journal of Natural Medicines 2023, **21**(10): 730-744
doi: 10.1016/S1875-5364(23)60466-2
Chinese Journal of Natural Medicines

•Special topic•

Tripterygium hypoglaucum extract ameliorates adjuvant-induced arthritis in mice through the gut microbiota

HU Jianghui[1Δ], NI Jimin[1Δ], ZHENG Junping[1], GUO Yanlei[2], YANG Yong[2], YE Cheng[3], SUN Xiongjie[1], XIA Hui[1], LIU Yanju[1*], LIU Hongtao[1, 2*]

[1] *College of Basic Medical Sciences, Hubei University of Chinese Medicine, Wuhan 430065, China;*
[2] *Chongqing Academy of Chinese Materia Medica, Chongqing 400065, China;*
[3] *Wuhan Customs Technology Center, Wuhan 430050, China*

Available online 20 Oct., 2023

[ABSTRACT] Traditionally, *Tripterygium hypoglaucum* (Levl.) Hutch (THH) are widely used in Chinese folk to treat rheumatoid arthritis (RA). This study aimed to investigate whether the anti-RA effect of THH is related with the gut microbiota. The main components of prepared THH extract were identified by HPLC-MS. C57BL/6 mice with adjuvant-induced arthritis (AIA) were treated with THH extract by gavage for one month. THH extract significantly alleviated swollen ankle, joint cavity exudation, and articular cartilage destruction in AIA mice. The mRNA and protein levels of inflammatory mediators in muscles and plasma indicated that THH extract attenuated inflammatory responses in the joint by blocking TLR4/MyD88/MAPK signaling pathways. THH extract remarkably restored the dysbiosis of the gut microbiota in AIA mice, featuring the increases of *Bifidobacterium*, *Akkermansia*, and *Lactobacillus* and the decreases of *Butyricimonas*, *Parabacteroides*, and *Anaeroplasma*. Furthermore, the altered bacteria were closely correlated with physiological indices and drove metabolic changes of the intestinal microbiota. In addition, antibiotic-induced pseudo germ-free mice were employed to verify the role of the intestinal flora. Strikingly, THH treatment failed to ameliorate the arthritis symptoms and signaling pathways in pseudo germ-free mice, which validates the indispensable role of the intestinal flora. For the first time, we demonstrated that THH extract protects joint inflammation by manipulating the intestinal flora and regulating the TLR4/MyD88/MAPK signaling pathway. Therefore, THH extract may serve as a microbial modulator to recover RA in clincial practice.ver RA in clincial practice.

[KEY WORDS] Arthritis; Gut microbiota; Immunity; Inflammation; *Tripterygium hypoglaucum*
[CLC Number] R965 **[Document code]** A **[Article ID]** 2095-6975(2023)10-0730-15

Introduction

Rheumatoid arthritis (RA) is an immune-mediated and joint-based chronic inflammatory autoimmune disorder affected by genetic and environmental factors, characterized by pain, stiffness, synovitis, and articular erosive destruction [1]. RA induces the proliferation of local tissue cells, synovial fibroblasts, and osteoclasts, which finally leads to irreversible damage to the cartilage and bone [2]. The worldwide prevalence of RA is about 1%, ranking among the top 15% of diseases that cause disability [3, 4].

Emerging evidence has demonstrated that the gut microbiota participates in the pathogenesis of RA *via* the intestinal flora-host immunity-joint axis. Under the physiological condition, intestinal bacteria help to maintain immune homeostasis in hosts by stimulating the production of immunoglobulin A (IgA) and promoting the maturation of regulatory T cells [5]. However, dysbiosis of the host renders hosts susceptible to joint diseases. RA patients were reported with enriched *Prevotella* in the gut, accompanied by reduced abundances of *Clostridia*, Lachnospiraceae, and *Bifidobacterium* [6, 7]. In contrast, regulating gut microbiota by diet or probiotics weakened inflammatory responses and slowed down the developoment of RA [8]. Clinically, patients with a five-year history of RA was greatly improved by fecal microbiota transplantation, which indicated the direct relationship between the gut microbiota and RA [9].

The gut microbiota affects the development of RA in

[Received on] 27-Apr.-2023
[Research funding] This work was supported by the Health Commission of Hubei Province of China (No. ZY2021Z005) and the Major Science and Technology Project in Yunnan Province (No. 202102AE090042).
[*]**Corresponding author]** E-mails: lyj1965954@hbtcm.edu.cn (LIU Yanju); hongtaoliu@hbtcm.edu.cn (LIU Hongtao)
[Δ]These authors contributed equally to this work.
These authors have no conflict of interest to declare.

multiple ways. For instance, the disturbed intestinal flora stimulateed the toll-like receptor 4/myeloid differentiation factor 88 (TLR4/MyD88) signaling pathway and induced T cell differentiation and maturation [10] . In addition, the colonic bacteria might elevate the phosphorylation of mitogen-activated protein kinases (MAPKs) containing c-Jun *N*-terminal kinase (JNK), P38, and extracellular regulated kinase 1/2 (ERK1/2), followed by activation of systemic inflammation [11]. The above evidence demonstrates that the gut microbiota may be an indispensable environmental factor that affects the pathogensis of RA.

Tripterygium hypoglaucum (Levl.) Hutch (THH) was originally recorded in *the Compendium of Materia Medica* by LI Shizhen. Traditionally, the roots of THH were used to treat RA or to ameliorate inflammation and pain in Chinese folk [12]. In previous studies, THH decoction potently inhibited inflammation, capillary permeability, exudation, and hyperplasia *in vivo* [13]. Furthermore, THH polyglycoside, one main chemical component, has proved to inhibit humoral immunity during the development of RA, as reflected by the decreased levels of serum IgA and IgM [14]. For oral administration, THH decoction will inevitably encounter intestinal microorganisms and may affect their community structure. However, no studies have focused on the possible role of the gut microbiota in THH-mediated protection against RA.

In the current study, we hypothesized that THH decoction improved the local inflammation of the joints by regulating the composition of the gut microbiota and their metabolic activities. To test this hypothesis, we prepared THH extract and analyzed its components by liquid chromatography-tandem mass spectrometry (LC-MS/MS). Based on the Complete Freund's adjuvant (CFA)-induced arthritis (AIA) mouse model, we evaluated the anti-arthritis performance of THH extract. Then, the regulatory effect of THH extract on the gut microbiota and joint damage was measured. Finally, the critical role of the gut microbiota was confirmed in pseudo-sterile mice treated with antibiotics.

Materials and Methods

Preparation of THH extract

Tripterygium hypoglaucum (Levl.) Hutch (THH) (Dechang, Sichuan, China, batch No. 20190401) was authenticated by Professor YANG Yong in Chongqing Academy of Chinese Materia Medica and deposited in Chongqing Academy of Chinese Materia Medica. The dried roots of THH were ground and decocted three times with five folds, four folds, and three folds of water at 60 °C, respectively. After the decoction was combined and filtered, the filtrate was concentrated to clear paste with a relative density of 1.05−1.07 at 60 °C. After the addition of ethanol (final 70%) and subsequent filtration, the filtrate was further concentrated to paste-like extract with a relative density of 1.20−1.25 at 60 °C. The THH extract was stored at −80 °C for further experiments. The chemical composition was identified by high-performance liquid chromatography (HPLC) and LC-MS/MS, and the details were depicted in Supplementary Methods.

Animal experiment

Male C57BL/6 mice (six weeks old, 20 ± 2 g) were purchased from Hubei Provincial Center for Disease Control and Prevention (Wuhan, China). The mice were acclimated for one week with a 12 h/12 h light/dark cycle (relative humidity, 55% ± 5%; temperature, 23 ± 2 °C) and free access to food and water. Then, the mice were randomly divided into four groups (n = 8): a Con group, an AIA group, a THH group, and an AIA + THH group. For mice in the AIA and AIA + THH groups, 100 μL of 1 mg·mL^{-1} CFA (Sigma, MO, USA) was subcutaneously injected into the right footpad using a microinjector (Beijing Envta Technology Co., Ltd., Beijing, China) on day one, while control mice were injected with 100 μL normal saline alone. Meanwhile, mice in the THH and AIA + THH groups were treated with THH extract (250 mg·kg^{-1}·d^{-1} by gavage) for 35 days. The animal experimental design is shown in Supplementary Fig. 1. In our preliminary study, both 125 and 250 mg·kg^{-1} of THH extract showed no observable toxicity on mice, and 250 mg·kg^{-1} of THH extract exerted better effectiveness. With respect to the human dosage of THH tablets (1.62 g·d^{-1}), the mouse dosage used in this study (250 mg·kg^{-1}·d^{-1}) was reasonable.

For pseduo-germ free experiments, male C57BL/6 mice were divided into four groups (n = 8): a Con group, an AIA group, an Ab + AIA group, and an Ab + AIA + THH group. During the whole experimental period, mice in the Ab + AIA and Ab + AIA + THH groups were given sterilized water with an antibiotic mixture (1.0 mg·mL^{-1} ampicillin, 1.0 mg·mL^{-1} neomycin sulfate, 0.5 mg·mL^{-1} vancomycin, and 0.5 mg·mL^{-1} metronidazole) (Aladdin, Shanghai, China) every day, while those in the other two groups were treated with normal sterilized water. From day 29, mice in the AIA, Ab + AIA, and Ab + AIA + THH groups were administered with CFA and THH extract, as described above. The animal experimental protocol was detailed in Supplementary Fig. 4A.

After treatment, the mice were euthanized by ether anesthesia and the major tissues were collected, including plasma, ankle, paw, ankle-adjacent muscle, intestinal tissue, and caecal contents. All samples were stored at −80 °C for further analysis. Animal experiments were conducted in accordance with the Ethical Experimentation Committee of Hubei University of Chinese Medicine (No. SCXK2020-0018).

Measurement of physiological and morphological indices

During the animal experiment, typical physiological indices of mice were monitored, such as ankle thickness, paw width, ankle circumference, and body weight. The arthritis scores were also recorded according to the criteria in Supplementary Table 1. The joint morphology was imaged using an

X-ray machine (Xi'an Institute of Optics and Mechanics, Xi'an, China), and the ankle thickness was measured by a digital thickness gauge (Guanglu Measuring Instruments Co., Ltd., Guangxi, China).

RNA extraction and quantitative real-time PCR (qRT-PCR)

Total RNA was extracted from muscle tissues (including synovial tissues) adjacent to mouse ankle using Trizol reagent (Summerbio, Beijing, China). The mRNA was reverse-transcribed into cDNA using the cDNA first-strand synthesis kit, according to the manufacturer's protocol (Summerbio, Beijing, China). The relative mRNA levels of target genes were detected by qRT-PCR using SYBR QPCR mixtures on an ABI 7500 real-time fluorescent quantitative PCR instrument system (Arlington, VA, USA). The reaction parameters were set as followed: 95 °C pre-denaturation for 10 min and 40 cycles of amplification (95 °C denaturation for 10 s, 60 °C annealing extension for 30 s). All the mRNA levels were normalized using *β*-actin as an internal control and the relative quantification of gene expression was calculated by the $2^{-\Delta\Delta Ct}$ method. The primer sequences are listed in Supplementary Table 2.

Determination of immunoglobulin and inflammatory cytokines in plasma

Immunoglobulins (IgG, IgM, and IgA) and cytokines (IL-1β, IL-6, and TNF-α) in plasma were quantified using ELISA kits, according to the manufacturer's instructions (Elabscience Biotechnology Co., Ltd., Wuhan, China). The absorbance was measured at 450 nm by a multi-scanning spectrum microplate reader (Molecular Devices Corporation, San Jose, CA, USA), and the concentration was calculated based on the standard curve.

Histopathological analysis

After the mice were sacrificed, the ankle joints stripped of joint-adjacent muscles were collected from the right hind-limb. The joints were fixed in 4% paraformaldehyde for 48 h and decalcified with 15% EDTA-Na_2 (pH 7.3) at room temperature for another 30 days. After sufficient decalcification, the tissues were embedded in paraffin and cut into 4 μm thick sections. Then, the sections were stained with hematoxylin-eosin (H&E) and Safranin-O/Fast green (SO) (Servicebio, Wuhan, China), respectively. Histopathological changes were observed under a Leica DMI4000B microscope (Wetzlar, Germany), and the images were captured by a Leica DFC310 FX digital camera (Wetzlar, Germany).

Western blot analysis

Total proteins from the right hind paw tissue of mice were extracted with RIPA lysis buffer supplemented with a protease inhibitor cocktail (Merck, Darmstadt, Germany). The protein concentration was determined using a BCA protein assay kit (Beyotime, Shanghai, China). Protein samples were separated on sodium dodecyl sulfate-polyacrylamide gel electrophoresis (SDS-PAGE) gel and transferred to polyvinylidene fluoride membrane. After blocking with 5% skim milk for 1 h, the membrane was incubated with primary antibodies at 4 °C overnight. Antibodies against MyD88, TLR4, p-P38, P38, p-ERK1/2, ERK1/2 and *β*-actin were purchased from Santa Cruz Biotechnology (Santa Cruz, CA, USA). Cyclooxygenase-2, superoxide dismutase 2, p-JNK and JNK were purchased from Cell Signaling Technology Inc. (Beverly, MA, USA). After washing, the membrane was incubated with horseradish peroxidase (HRP)-conjugated secondary antibodies (Cell Signaling Technology, Danvers, MA, USA). The protein bands were visualized using ECL luminescent solution (Cell Signaling Technology, MA, USA), and the densitometry was quantified with Image J2x software (National Institute of Health, Bethesda, MD, USA).

16S rDNA sequencing and gut microbiota analysis

Fecal genomic DNA was extracted from 32 fecal samples using the Fast DNA™ SPIN kit (MP Biomedicals, CA, USA) for intestinal flora analysis. The V3-V4 region of 16S rDNA was sequenced on the Illumina MiSeq platform (Illumina, San Diego, CA, USA). Linear discriminant analysis of effect size (LEfSe), Phylogenetic Investigation of Communities by Reconstruction of Unobserved States (PICRUSt), and Spearman's correlation analysis were performed to further analyze the compositional and functional variation of the gut microbiome [15, 16]. The details are provided in Supplementary Methods.

Statistical analysis

Data were analyzed by GraphPad Prism version 8.02 software (GraphPad Software, Inc, San Diego, CA, USA) and are expressed as the mean ± SD. Statistical significance was evaluated by the one-way analysis of variance (ANOVA) with Bonferroni post-hoc analysis among experimental groups. LEfSe analysis was performed based on Kruskal-Wallis and Wilcoxon test. A P value less than 0.05 was considered to be statistically significant.

Results

Component identification of THH extract

To identify the authenticity of THH, triptolide in THH extract was analyzed as recorded in *the Chinese Pharmacopoeia* (2020 edition). The HPLC spectrum showed that the retention time (t_R) (47.471 min, Supplementary Fig. 2A) of the major peak in THH extract was similar to that of triptolide standard (47.323, Supplementary Fig. 2B), indicating the authenticity of THH herb in this study. Furthermore, a total of nine components of THH extract were identified by HPLC-MS/MS in multiple reaction monitoring modes (Fig. 1A and Supplementary Fig. 3). These components were determined to be terpenoids (such as triptolide and tripterine) and alkaloids (such as wilfortrine and wilforgine) (Supplementary Table 3).

Effect of THH extract on the physiological indices of AIA mice

Relevant physiological indices were monitored to assess the therapeutic effect of THH extract on arthritic mice. In comparison with the Con group, the AIA group showed significant increases in ankle thickness, claw width, and ankle cir-

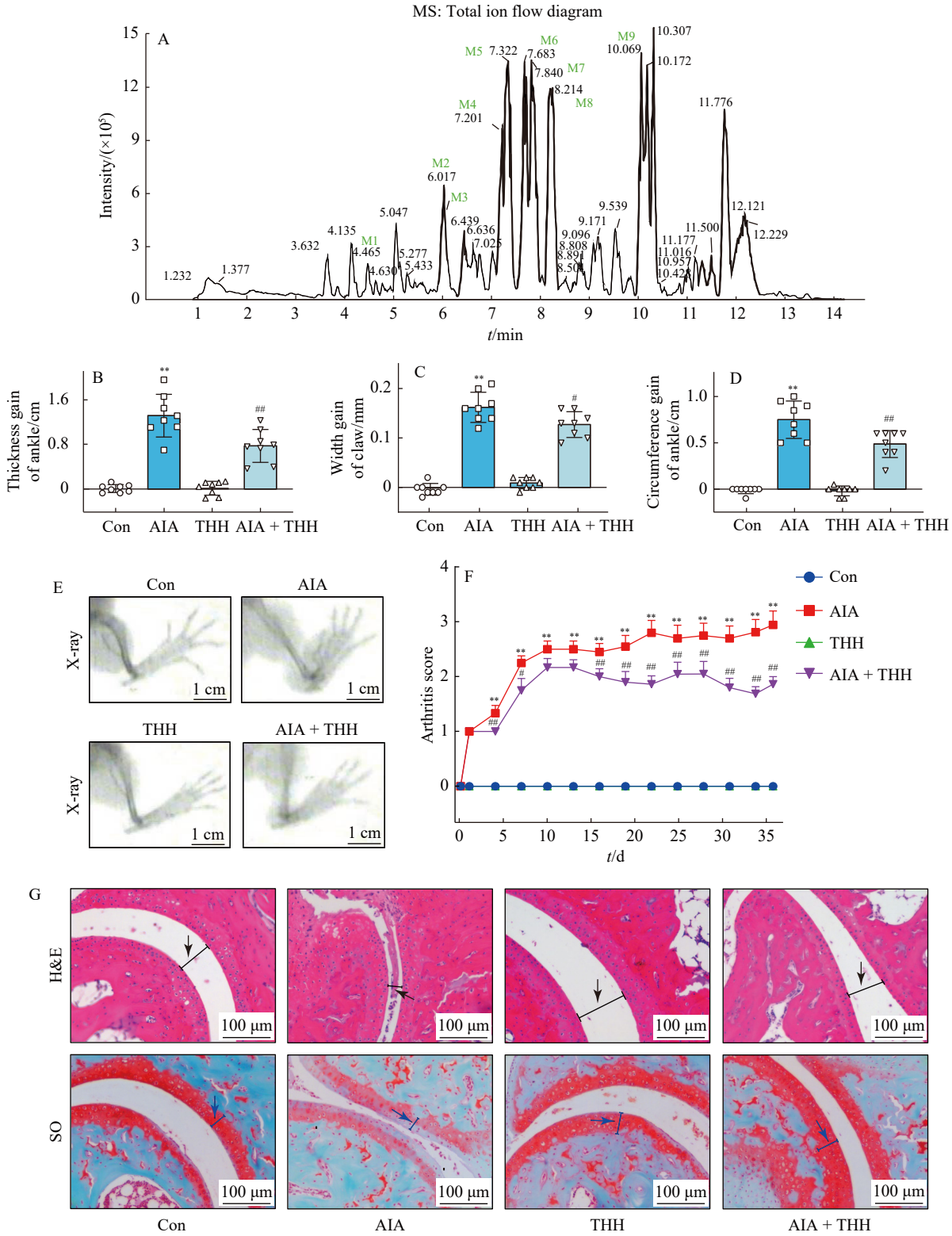

Fig. 1 THH extract's composition and its effect on AIA mice. (A) Total ion flow diagram of THH extract using UPLC-MS analysis. M1, wilforlide B; M2, wilforidine; M3, triptolide; M4, wilformine; M5, wilfortrine; M6, wilfordine; M7, wilforgine; M8, wilforine; and M9, tripterine. During THH extract treatment (250 mg·kg^{-1}·d^{-1}), the physiological indices of mice were monitored, including ankle thickness (B), paw width (C), ankle circumference (D), the severity of ankle swelling (E), and arthritis score (F) in four experimental groups. (G) H&E and SO staining analyses of ankle joint tissues. Black arrows indicate the width of joint cavity. Blue arrows indicate the content of articular cartilage. Data are expressed as the mean ± SD (n = 8). $^{**}P < 0.01$ *vs* the Con group; $^{\#}P < 0.05$, $^{\#\#}P < 0.01$ *vs* the AIA group.

cumference ($P < 0.01$, *vs* the Con group), which were statistically reversed after THH extract treatment ($P < 0.05$ or 0.01, *vs* the AIA group) (Figs. 1B–1D). As revealed by X-ray imaging, the severity of swollen soft tissues in the ankle and paw joint was remarkably ameliorated after THH extract treatment (Fig. 1E). According to arthritis scores, THH extract suppressed the development of arthritis in CFA-treated mice ($P < 0.01$, *vs* the AIA group), and THH extract itself had no impact on arthritis scores in control mice (Fig. 1F). Furthermore, H&E staining illustrated that joint space was notably narrowed in the AIA group (Fig. 1G). In addition, SO staining suggested the loss of cartilage proteoglycan (stained in red) in the AIA group (Fig. 1G). In contrast, THH extract treatment alleviated the reduction of joint space, the exudation of joint cavity, and the destruction of articular cartilage. These results suggest that THH extract significantly ameliorates the histopathological damage to the joints in AIA mice.

Suppressive effect of THH extract on immune activation in AIA mice

Furthermore, we detected the transcriptional expression of pro-inflammatory cytokines and the secretion of immunoglobulins in the four experimental groups. As indicated in Fig. 2A, the mRNA levels of interleukin-1β (*IL-1β*), tumor necrosis factor-α (*Tnf-α*), *Il-8*, cyclooxygenase-2 (*Cox-2*), monocyte chemotactic protein-1 (*Mcp-1*), and *Il-6* increased in the synovial tissues of AIA mice ($P < 0.01$, *vs* the Con group), which were significantly reversed after treatment with THH extract ($P < 0.05$ or 0.01, *vs* the AIA group). In contrast, THH extract statistically inhibited the down-regulation of *IL-10* mRNA (an anti-inflammatory cytokine) ($P < 0.05$, *vs* the AIA group) (Fig. 2A).

Next, the secretion of immunoglobulins (IgG, IgM, and IgA) and pro-inflammatory cytokines (IL-1β, TNF-α, and IL-6) in plasma were measured by ELISA. The results suggested that these factors except IL-1β were elevated in the AIA group ($P < 0.05$ or 0.01 *vs* the Con group), whereas their activation was effectively blocked by THH extract treatment ($P < 0.05$ or 0.01, *vs* the AIA group) (Figs. 2B and 2C).

Modulatory effect of THH extract on inflammation-related regulators

Evidence shows that TLR4 plays an important role in inducing synovial inflammation and arthritis [17]. To decode the molecular mechanism driving THH extract to prevent AIA in mice, the key proteins responsible for the immune regulation were detected by Western blot. As demonstrated in Fig. 3, the levels of TLR4, MyD88, COX-2, SOD2, p-P38, p-ERK1/2, and p-JNK remarkably increased in the paw of AIA mice, where the elevation of TLR4, COX-2, SOD2, p-P38, and p-JNK was significantly inhibited by THH extract treatment (Figs. 3A–3E).

Remodelling of gut microbiota structure of AIA mice by THH extract

Intestinal flora imbalance is closely associated with the

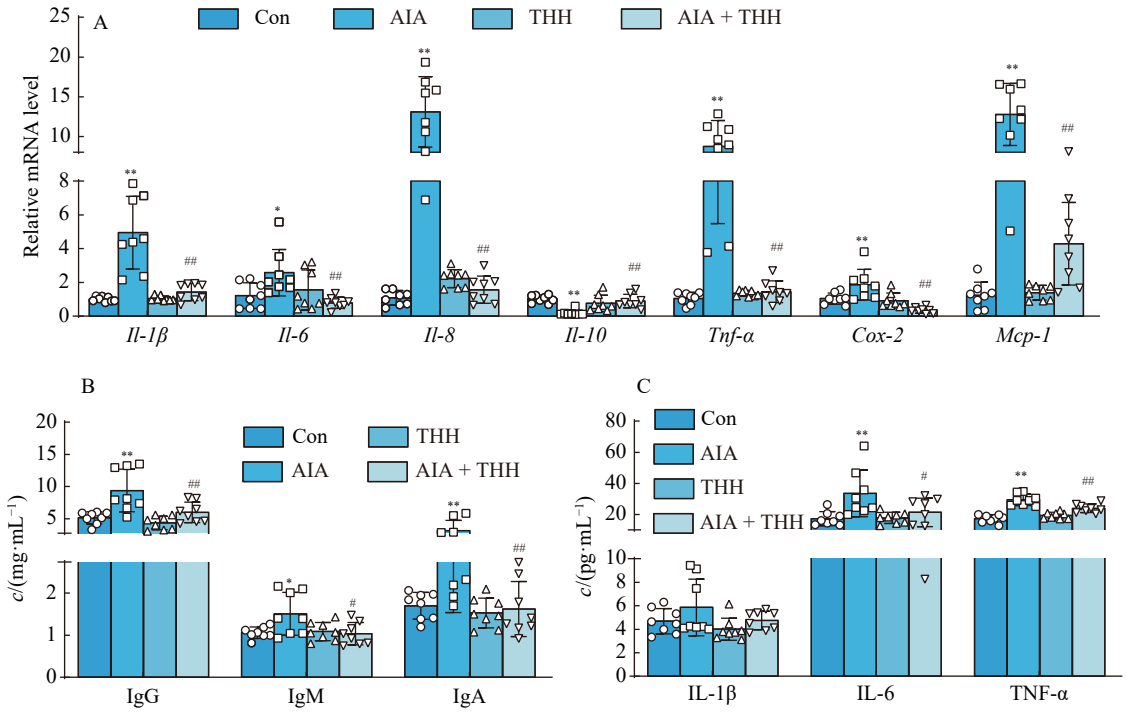

Fig. 2 THH extract inhibits immune activation in AIA mice. (A) The mRNA levels of inflammatory cytokines in ankle-adjacent muscle tissues (including synovial tissues) by qRT-PCR, including *Il-1β*, *Tnf-α*, *Il-8*, *Il-10*, *Cox-2*, *Mcp-1*, and *Il-6*. (B) Plasma immunoglobulins including IgG, IgM, and IgA. (C) Protein levels of pro-inflammatory cytokines in plasma, including IL-1β, TNF-α, and IL-6. Data are expressed as the mean ± SD ($n = 8$). $^{*}P < 0.05$, $^{**}P < 0.01$ *vs* the Con group; $^{\#}P < 0.05$, $^{\#\#}P < 0.01$ *vs* the AIA group.

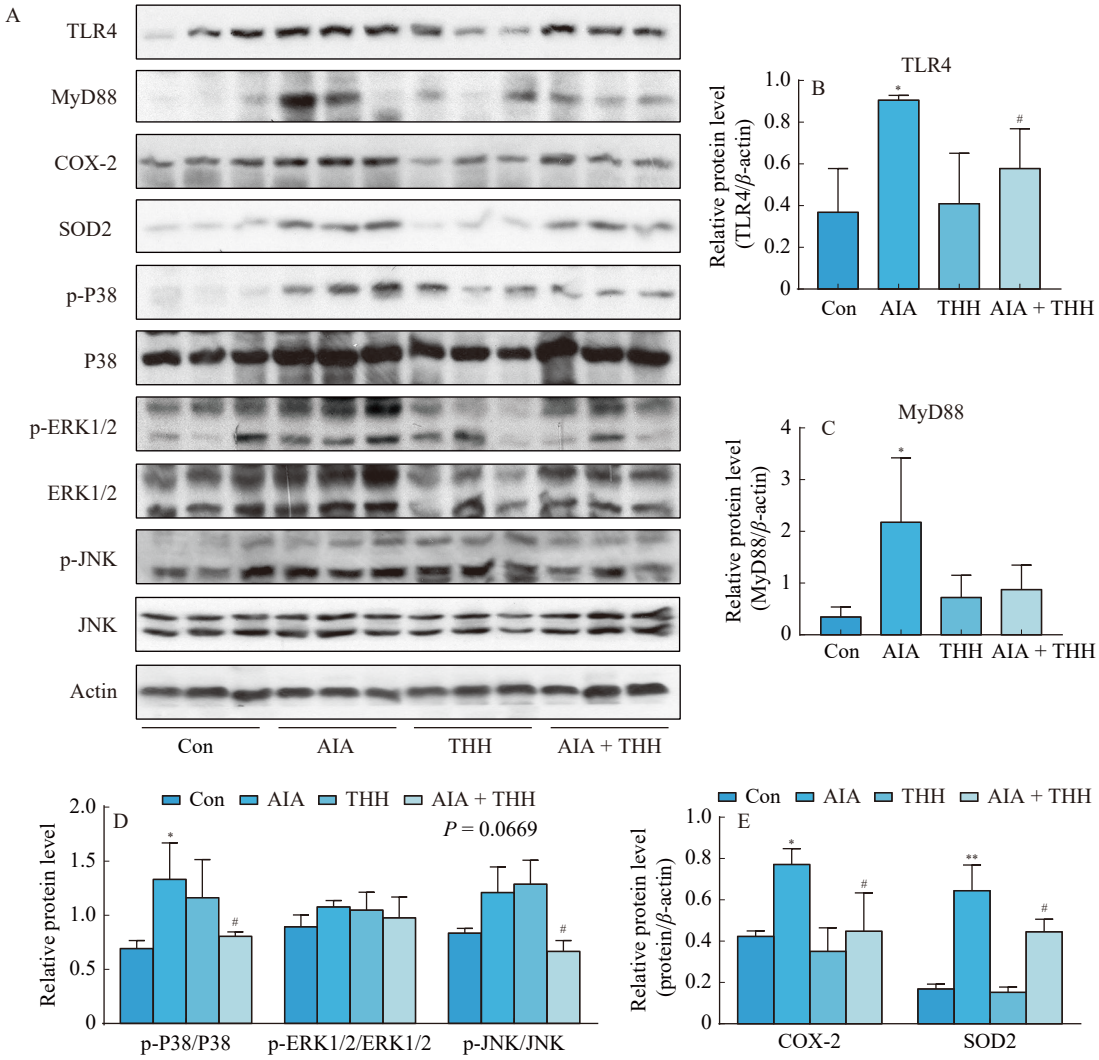

Fig. 3 THH extract reverses the up-regulation of inflammation-related regulators in AIA mice. (A) Protein expression of TLR4, MyD88, COX-2, SOD2, p-P38, P38, p-ERK1/2, ERK1/2, p-JNK and JNK in paw tissues by Western blot. (B-E) Quantitative analysis of the protein bands in (A). Data are expressed as the mean ± SD (n = 8). $^{*}P < 0.05$, $^{**}P < 0.01$ *vs* the Con group; $^{\#}P < 0.05$ *vs* the AIA group.

occurrence of RA [18]. To investigate the regulatory effect of THH extract on the gut microbiota, 32 fecal samples from the four experimental groups were analyzed by 16S rDNA sequencing. The Multy samples Shannon−Wiener curves revealed that 16S rDNA sequencing generated enough data for analyzing microbial composition (Fig. 4A). In addition, the complete separation of intestinal flora clusters in principal coordinate analysis (PCoA) depicted that THH extract exerted significant effect on the intestinal flora structure (Fig. 4B).

At the phylum level, THH extract significantly enhanced the abundances of Firmicutes, Verrucomicrobia, and Actinobacteria and reduced the levels of Bacteroidetes and Proteobacteria in AIA mice (Fig. 4C). At the family level, THH extract reduced the contents of Bacteroidales S24-7 group, Prevotellaceae, and Rikenellaceae but elevated the abundances of Lachnospiraceae, Erysipelotrichaceae, and Lactobacillaceae in AIA mice (Fig. 4D).

To figure out the microbial alteration at the genus level, 30 bacteria with the greatest variation were displayed in a heatmap. Among them, six bacteria increased in AIA mice including *Butyricimonas*, *Parabacteroides*, *Bacteroides*, *Desulfovibrio*, *Anaeroplasma*, and *Marvinbryantia*, which were significantly repressed by THH extract (Fig. 4E). On the contrary, over twenty bacteria decreased in the AIA group compared with those of the Con group, such as *Bifidobacterium*, *Lactobacillus*, *Akkermansia*, *Turicibacter*, *Faecalibaculum*, and *Ruminiclostridium* (Fig. 4E). Most of them were effectively restored by THH extract treatment (Fig. 4E). The abundance quantification of these genera is presented in Supplementary Fig. 4.

To determine the specific bacterial taxa in each experimental group, LEfSe analysis was performed. As depicted in the branching diagram, Rikenellaceae, Prevotellaceae, Helicobacteraceae, and Desulfovibrionaceae families dominated the AIA group, whereas there were several families that greatly contributed to the gut microbiota community in the

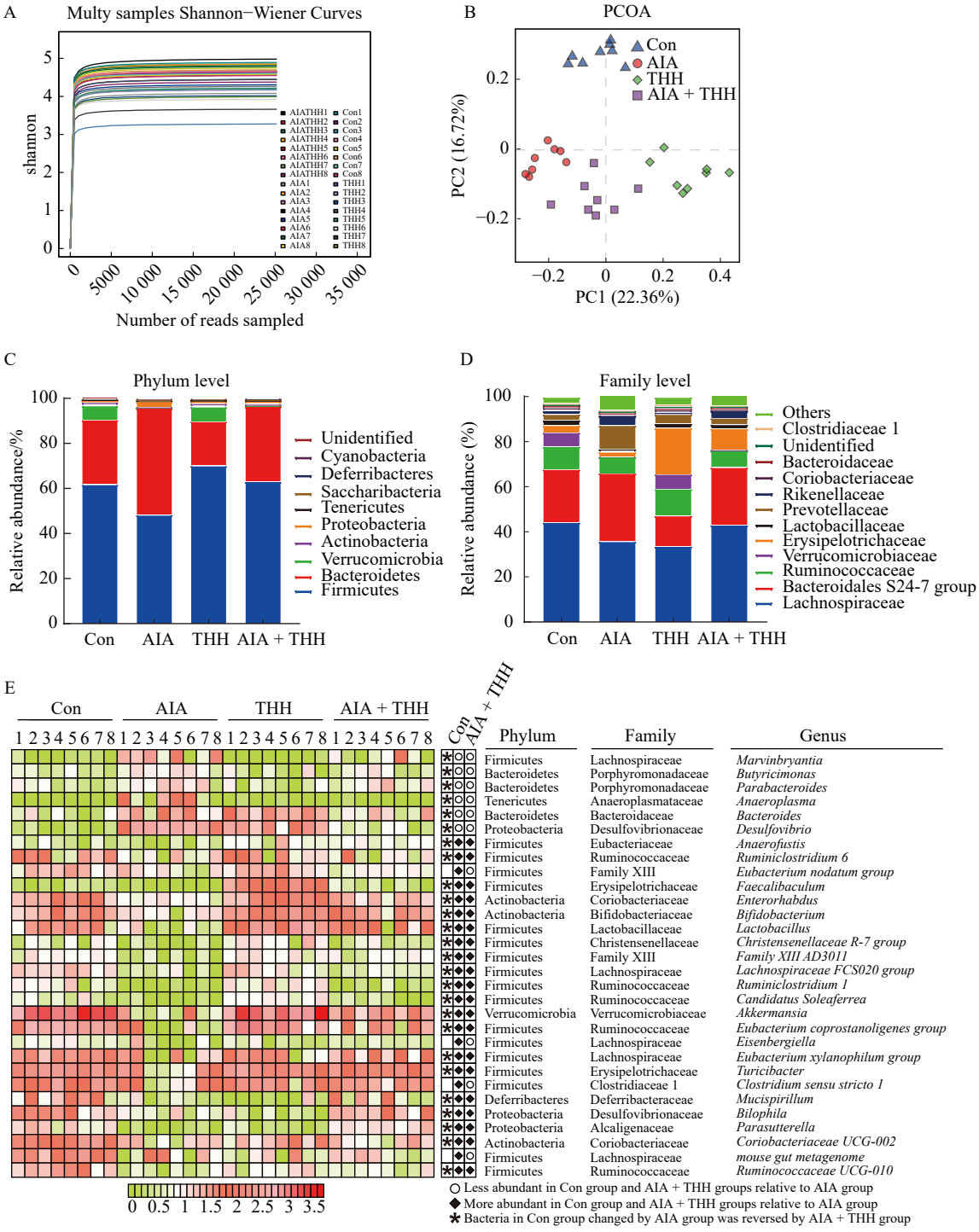

Fig. 4 Improvement of THH extract on gut microbiota imbalance in AIA mice. After THH extract treatment, all the mice were euthanized and their caecal samples were collected for 16S rDNA sequencing analysis. (A) Multy samples Shannon−Wiener curves during microbial sequencing. (B) Beta diversity using principal co-ordinate analysis (PCoA). (C) Abundance changes of the gut microbiota at the phylum level. (D) Abundance changes of the gut microbiota at the family level. (E) Bacteria with the greatest variation at the genus level were displayed in a heatmap.

THH group, namely Bifidobacteriaceae, Verrucomicrobiaceae, Oxalobacteraceae, and Erysipelotrichaceae (Fig. 5A). As for the AIA + THH group, Enterococcaceae was the representative family (Fig. 5A). Furthermofd, LDA scores were calculated to identify the characteristic genera of each group: *Lachnosplraceee NK4A136 group*, *Corynebacterium 1* and *Ruminococcaceae UCG 007* for the Con group; *Alloprevotella* and *Alistipes* for the AIA group; *Akkermansia* for the THH group; and *Roseburia*, *Lachnospiraceae UCG 010*, and *Odoribacter* for the AIA + THH group (Fig. 5B).

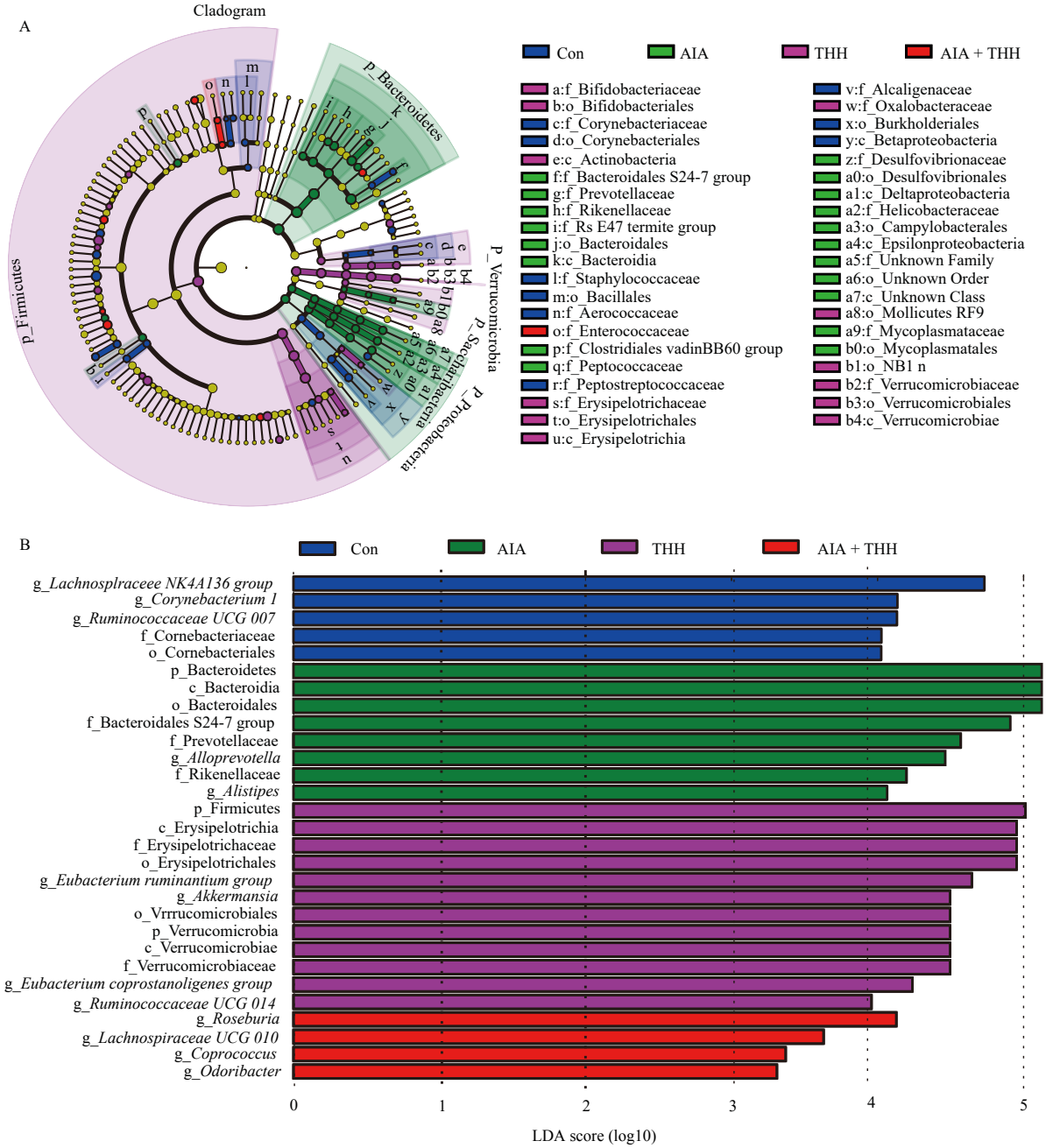

Fig. 5 Identification of the characteristic taxa in the four experimental groups by linear discriminant analysis (LDA) effect size (LEfSe). (A) Taxonomic abundance of enriched taxa using LEfSe. The dot size is proportional to the relative abundance of enriched bacterial taxa ("c", class; "o", order; "f", family). Circles radiating from the inside out represent taxonomic levels from phylum to genus (or species). (B) Most significant differences of intestinal bacterial taxa among the experimental groups after LDA using a threshold score larger than 3.0. The bar length represents the impact of significantly different species among the experimental groups.

Metabolic pathway regulation of the gut microbiota in AIA mice by THH extract

To explore the potential effect of THH extract on the metabolic pathways of the gut microbiota, a phylogenetic study of the intestinal flora was conducted using PICRUSt analysis based on the KEGG (Kyoto Encyclopedia of Genes and Genomes) database. The results showed that several metabolic pathways of the gut microbiota were changed in AIA mice ($P < 0.05$ or 0.01 *vs* the Con group) (Fig. 6A). Among them, eight pathways were greatly upregulated (such as Lipopolysaccharide biosynthesis and Lipoic acid metabolism), while seven pathways were downregulated (such as Starch and sucrose metabolism, Pentose phosphate pathway and Galactose metabolism, and Pyruvate metabolism). In contrast, most of these altered pathways were restored in the AIA + THH group ($P < 0.05$ or 0.01 *vs* the AIA group) (Fig.

6B). To examine the correlation between the gut microbiota and joint inflammation, the microbial metabolites were analyzed, including short-chain fatty acids, indole, and 5-hydroxytryptamine (5-HT) (Supplementary Fig. 5). The results showed that THH treatment elevated the contents of acetic acid and pentanoic acid in the intestine of AIA mice (Supplementary Fig. 5A). THH treatment suppressed the levels of indole in AIA mice, without effect on the abundance of 5-HT (Supplementary Figs. 5B−5C).

Correlation between physiological indicators and the gut microbiota

To illustrate the relationship between gut microbiota regulation and arthritis improvement, Spearman's correlation analysis was performed. As demonstrated in Fig. 6C, most of the altered genera were significantly associated with AIA-related physiochemical traits, such as joint swelling and arthritis scores, immune response, inflammation, and oxidative stress. For instance, several bacteria such as *Marvinbryantia*, *Desulfovibrio*, *Parabacteroides*, and *Butyricimonas* were positively correlated with pathological indicators, while some other bacteria such as *Bifidobacterium*, *Akkermansia*, *Lactobacillus*, and *Faecalibaculum* were negatively correlated with arthritis pathology.

Effect of THH extract on AIA mice with gut microbiota depletion

To further investigate the role of the gut microbiota against arthritis, mice with gut microbiota deleted were used for further studies (the procedures involved are presented in Supplementary Fig. 5A). After Abx treatment for four weeks, the intestinal tract of the mice was almost bare of bacteria (Supplementary Table 4), indicating that Abx-treated mice were qualified to establish a pseudo germ-free model (Supplementary Figs. 6B–6F). The combination of the four antibiotics also reduced water intake (Supplementary Fig. 6G). Interestingly, THH extract failed to recover the pathological changes in Abx-treated AIA mice, like ankle swelling, joint space narrowing, and high arthritis score (Figs. 7A–7F). Furthermore, the expression of inflammation-related cytokines in the synovial tissues of Abx-treated AIA mice was not reversed by THH extract, including *Il-1β*, *Il-8*, *Il-10*, *Tnf-α*, and

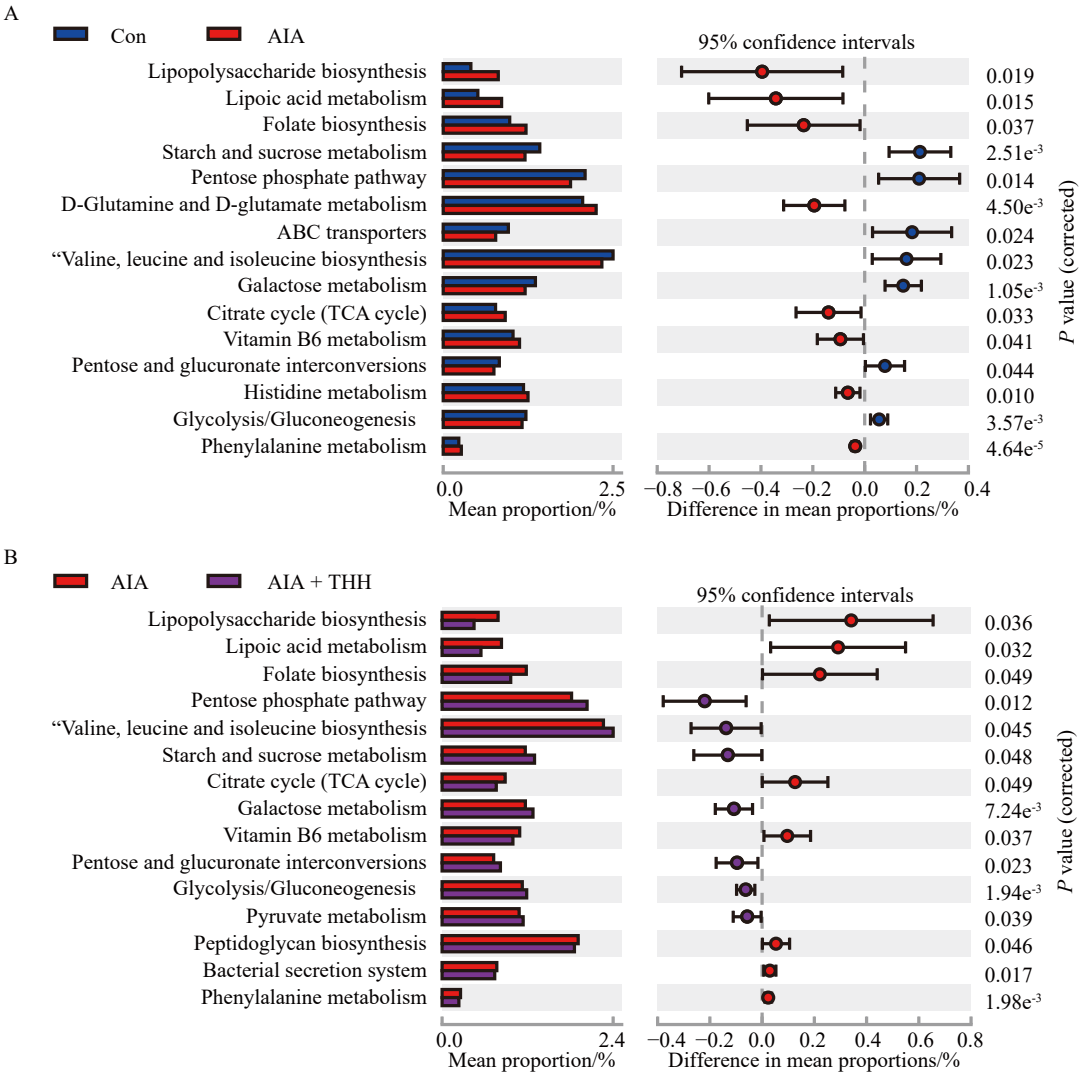

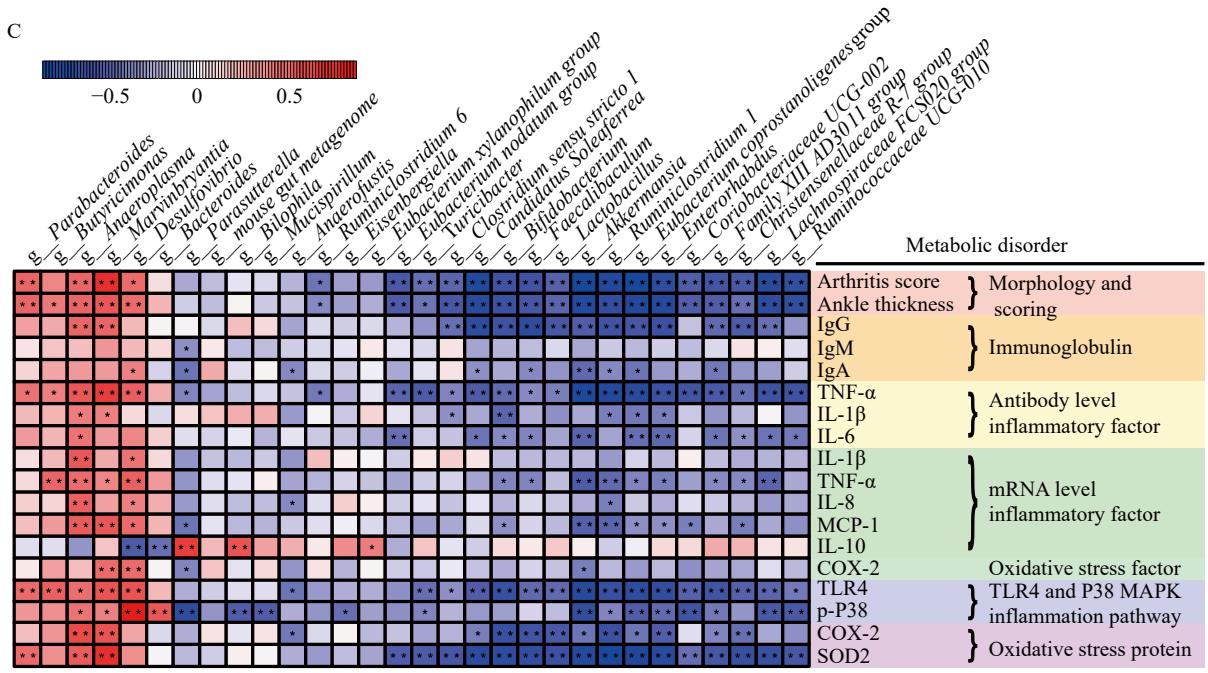

Fig. 6 Predicted metabolic pathways and correlation analysis between physiological indicators and altered intestinal bacteria. (A) Alteration of KEGG (Kyoto Encyclopedia of Genes and Genomes) pathways of the gut microbiota in AIA mice versus Con mice. (B) Reversal of KEGG pathway changes in AIA mice after THH extract treatment. (C) Spearman's correlation between altered bacteria and arthritis-related traits was analyzed at the genus level. Statistical significance is indicated with asterisks ($^{*}P < 0.05$, $^{**}P < 0.01$). Correlation coefficient is presented as color from blue (−1) to red (1), corresponding to negative and positive relationship.

Cox-2 (Figs. 8A–8E). Also, THH extract did not suppress the upregulation of signaling regulators in the ankle tissue of germ-free AIA mice, such as TLR4, MyD88, p-P38, p-ERK1/2 and p-JNK (Supplementary Fig. 7).

Discussion

Rheumatoid arthritis (RA) is characterized by synovial inflammation and destruction of the joint cartilage and bone mediated by the persistent production of proinflammatory cytokines. In the past, many Chinese herbals displayed potent effect on RA, such as *Tripterygium hypoglaucum* [12], *Tripterygium wilfordii* [19], and *Atractylodis* rhizome [20]. So far, Huobahuagen tablet, prepared from THH, has been widely used for the treatment of RA in China. However, it remains elusive about the underpinning mechanism of THH against RA. In this study, we confirmed the pivotal role of the gut microbiota in the improvement on arthritis and in the regulation of inflammation-related signaling pathways.

THH is a traditional Chinese medicine commonly used for autoimmune diseases [12]. In this study, we identified the major components of THH extract (Fig. 1A, Supplementary Figs. 2–3), and the results were consistent with a previous study where 116 chemical compounds were detected from THH extract, such as wilforine, wilfortrine, and triptolide [21]. Moreover, triptolide and tripterine were found to be the main active ingredients of THH against RA [22]. Triptolide exerted potent anti-inflammatory, immunosuppressive, anticancer, and anti-arthritic activities [23]. From the structure-efficacy perspective, triptolide is extremely similar with hydrocortisone: a clinically used anti-inflammatory drug for the treatment of autoimmune diseases such as rheumatoid arthritis. Consistently, triptolide-riched THH exerted significant anti-inflammatory and immunomodulatory effect in our study. In addition, we also identified several alkaloids such as wilforine, wilfordine, and wilforgine, which were reported to be bioactive components of THH extract [24]. These alkaloids were also found in healthy mouse feces after oral administration of tripterygium glycosides [25], suggesting the possible interaction of THH extract with the gut microbiota.

The CFA-induced arthritis animal model shares common features with human RA like joint swelling, synovial inflammation, and cellular infiltration [26]. In addition to rat arthritis models, previous researchers also used C57BL/6 mice for CFA-induced arthritis modeling [27, 28]. In this study, typical RA symptoms were observed in CFA-treated mice, indicating the success of adjuvant-induced arthritis modeling in C57BL/6 mice. These symptoms were significantly improved by THH extract (Fig. 1), suggesting the efficacy of THH extract against arthritis.

The pivotal event of RA is synovial inflammation and proliferation, which finally leads to the destruction of the cartilage, joint, and bone. During the pathogenesis of synovitis, inflammatory cells infiltrate into the synovial membrane and produce a wide range of chemokines [29]. Consistently, the

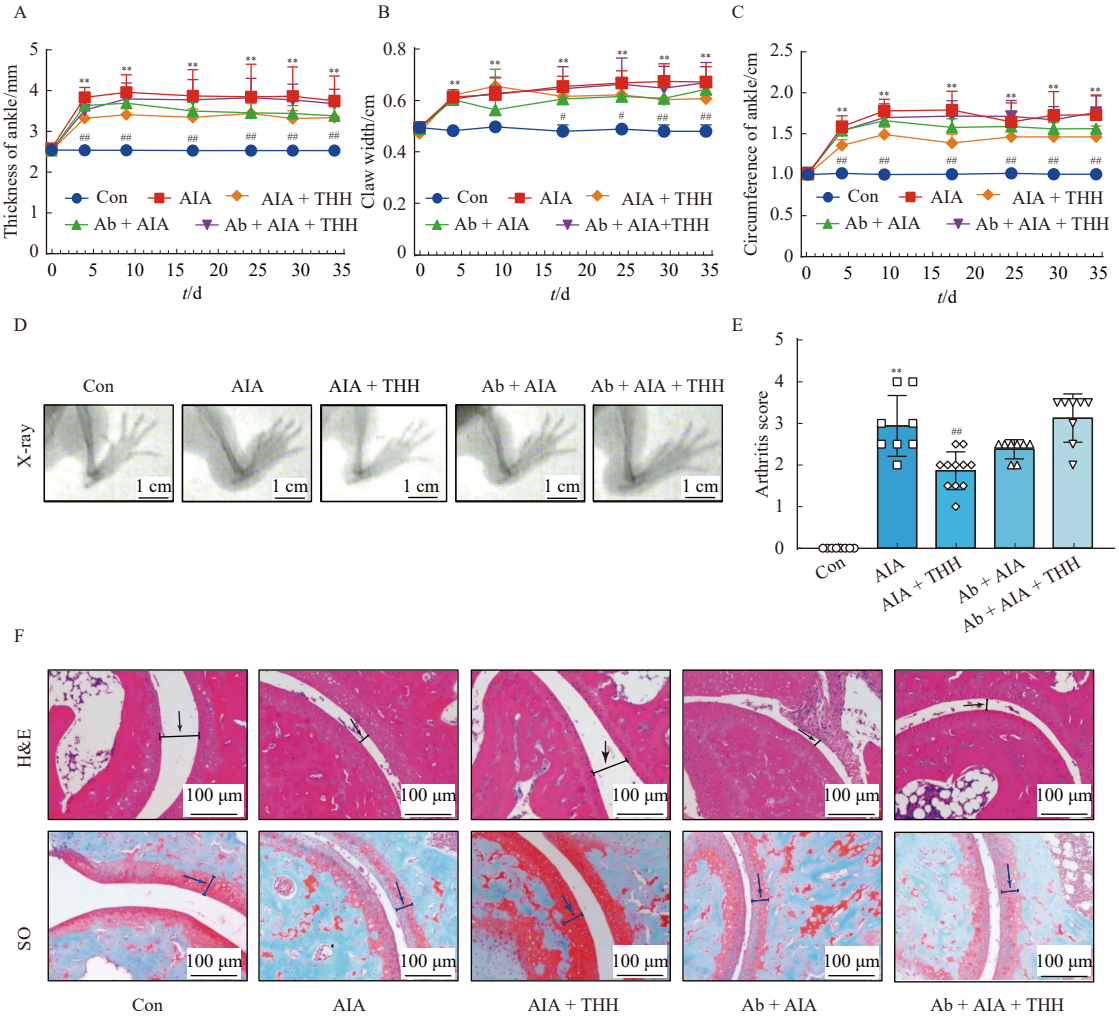

Fig. 7 THH extract fails to improve arthritis in AIA mice with gut microbiota deleted by Abx treatment. During THH extract treatment (250 mg·kg^{-1}·d^{-1}), the physiological indices were monitored, including ankle thickness (A), claw width (B), ankle circumference (C), X-ray imaging and paw tissues (D), and arthritis score of the right hind limb (E). After THH extract treatment, the mice were euthanized and the ankle joint tissues were collected for H&E and SO stainings (F). Black arrow indicates the width of joint cavity. Blue arrow indicates the content of articular cartilage. Data are expressed as the mean ± SD (n = 8). $^{**}P$ < 0.01 *vs* the Con group.

overwhelming release of TNF-α, IL-6, IL-8, and IL-1β was detected in serum and synovial fluid from RA patients. [30] These pro-inflammatory cytokines further induced osteoclastogenesis and bone erosion by acting on osteoclast precursors [31]. In parallel, our work validated the suppression of inflammation in the synovial membrane of AIA mice by THH extract (Fig. 2A). Besides, THH extract reduced the levels of immunoglobulins (IgG, IgM, and IgA) in the serum of AIA mice (Fig. 2B). Immunoglobulins are important mediators of acquired immunity, and the high titers of immunoglobulins in individuals were reported to be associated with persistent severity of inflammatory polyarthritis [32]. The above results indicate that THH extract exert pronounced inhibitory effect on both inflammatory responses and humoral immunity in AIA mice.

As pattern recognition receptors, TLRs are widely expressed in immune cells for recognizing pathogen-associated molecular patterns (PAMPs) and activating MyD88, highly expressed in the synovial tissue of RA patients [33]. TLRs are involved in the pathological process of RA by inducing downstream inflammation. Increasing evidence has shown that TLR4 is responsible for regional joint inflammation, cartilage proteoglycan depletion and bone erosion [34]. Deletion or loss-of-function mutation of *Tlr4* protected mice against drug-induced arthritis [35]. As the downstream of TLRs, MAPK proteins including P38, ERK, and JNK remained phosphorylated in fibroblast-like synoviocytes from RA patients or mice [36]. Here, we found that THH extract not only significantly downregulated the levels of TLR4, COX-2, and SOD2, but also obviously blocked the activation of P38 and JNK in AIA mice (Fig. 3). Likewise, triptolide (a major component of THH) was proved to inhibit the TLR4/MyD88 sig-

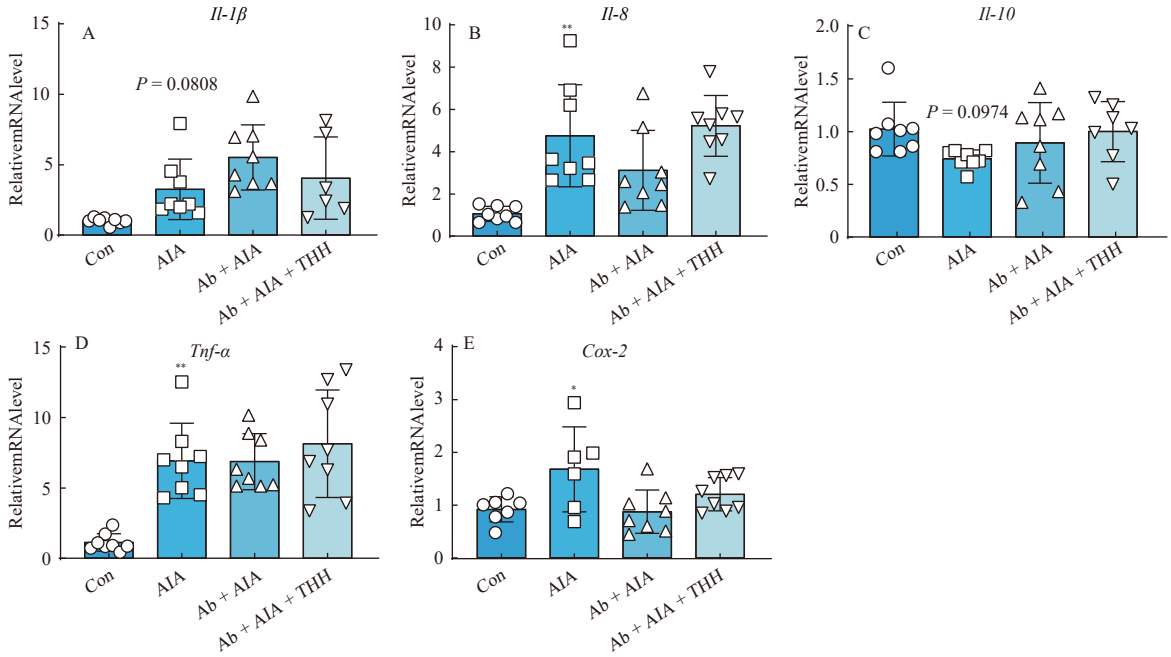

Fig. 8 THH extract exerts no suppressive effect on inflammatory responses in the ankle tissues of AIA mice with gut microbiota depleted. The mRNA expression of *Il-1β* (A), *Il-8* (B), *Il-10* (C), *Tnf-α* (D) and *Cox-2* genes (E) in synovial muscles adjacent to ankle joint was detected by qRT-PCR. Data are expreaaed as the mean ± SD (n = 8). $^{*}P < 0.05$, $^{**}P < 0.01$ *vs* the Con group.

naling pathway in LPS-treated macrophages [37]. Hence, we proposed that THH extract may treat arthritis by blocking the response of the TLR4/MyD88/MAPK signalling pathway, thereby inhibiting inflammatory reactions and oxidative stress in articular tissues.

The mutual interaction between the gut microbiota and the host immune system affects the progress of RA [38]. In RA patients, gut dysbiosis reflected different serological and clinical parameters [39]. Dysbiosis of the gut may contribute to the occurrence of RA *via* the gut-joint axis [40], which is maintained by gut barrier, immune cells, and microbiota-derived metabolites [40]. For example, microbial dysbiosis-induced dysregulation of short-chain fatty acids (SCFAs) led to immune activation and inflammation in RA [41]. In our work, the microbial dysbiosis should be the consequence of AIA (Fig. 4B), as the arthritis model was established by CFA through subcutaneous injection rather than oral administration. Furthermore, the dysbiosis may deteriorate the development of arthritis. Pathogenic bacteria and their toxins directly invaded the intestinal mucosa, damaged the intestinal barrier, and induced the imbalance of systemic immunity and the subsequent onset of RA [42]. The alteration of intestinal flora stimulated immune cells (e.g., T cells) in submucosal Peyer's plaques and then triggered systemic immune response *via* multiple pathways [43]. The Firmicutes/Bacteroidetes (F/B) ratio was negatively correlated with IgG and IgM levels in hosts [44], and most members of the phylum Proteobacteria were validated to be inflammatory inducers *in vivo* [45]. THH extract increased the F/B ratio and diminished Proteobacteria abundance in AIA mice, which was in line with the changes in IgG and inflammatory inducers. THH extract statistically reversed most of the changed genera in AIA mice (Fig. 4E). Among those reduced genera by THH extract, *Marvinbryantia* was positively associated with intestinal inflammation [46]; *Desulfovibrio*, an LPS producer and sulfate-reducing bacteria, colonized in the human gut and triggered the shift of the gut microbiota from homeostasis to inflammation [47]. Interestingly, THH extract remarkably increased the abundances of several beneficial genera such as *Akkermansia*, *Bifidobacterium*, and *Lactobacillus*. These probiotics are short-chain fatty acids (SCFAs) producers, and the SCFAs may reverse the gut dysbiosis and subside excessive inflammation through signaling pathways [48]. For instance, a mixture of *Lactobacillus* and *Bifidobacterium* was used to reduce inflammatory biomarkers and oxidative stress in RA patients [49]. More specifically, *Lactobacillus rhamnosus* GG inhibited oxidative stress and inflammation by downregulating the MAPK and TLR4/MyD88 pathways *in vivo* and *in vitro* [50]; loss of *Bifidobacterium* resulted in systemic inflammation and macrophages infiltration into the synovium [51]. Particularly, *Lactobacillus* and *Bifidobacterium* were proven to regulate bone homeostasis and to prevent bone loss [52]. Furthermore, LEfSe analysis showed that THH not only fundamentally regulated *Roseburia* and *Odoribacter* in AIA mice, but also strongly stimulated *Akkermansia* in control mice (Fig. 5B). Among them, the genus *Roseburia* was reported to possess butyrate-producing and anti-inflammatory properties [53]. *Roseburia* was substantially less in RA patients [54]. These three bacteria

were observed to be substantially declined in RA patients [54-56]. Consistently, THH treatment upregulated the contents of acetic acid and pentanoic acid, and both SCFAs were validated to block arthritis [57, 58]. Moreover, Spearman correlation analysis suggested that the above changed bacterial genera were closely correlated with RA-related physiological parameters or biomarkers (Fig. 6C).

Alternation of the gut microbiota affects the onset and development of RA. As a typical example, germ-free mice are resistant to spontaneous RA modeling, but can be developed into RA after segmented filamentous bacteria treatment [59, 60]. Germ-free mice presented severer arthritis symptoms after fecal microbiota transplantation (FMT) from mice susceptible to CIA [61]. Consistently, we found that depletion of the gut microbiota did not attenuate CFA-induced AIA (Fig. 7), and the reason may be that antibiotics treatment blocked the growth of both beneficial and detrimental bacteria. A previous study indicated that germ-free rats had higher susceptibility to adjuvant-induced arthritis than conventional rats [62]. The intestinal bacteria-deprived mice were partly reflected with loss of *Akkermansia*, *Bifidobacterium*, *Bacteroides*, and other altered bacteria (Supplementary Fig. 5). Finally, depletion of the intestinal flora from AIA mice confirmed that the amelioration of RA by THH extract was dependent on the presence of the intestinal flora (Fig. 7, Fig. 8 and Supplementary Fig. 6). For more detailed mechanisms, the altered gut microbiota may generate less inflammatory initiators (such as LPS) and more beneficial metabolites to manipulate immune and metabolic pathways [63]. THH extract is able be transformed by altered microbiota into active components for alleviating joint inflammation [64]. To fully explore the direct evidence for the specific contribution of the gut microbiota, more data on metabolic molecules and FMT should be provided in our future study. The alteration of microbial metabolites (LPS) and THH components may collectively modulate the TLR4-meidated inflammatory responses in the joints. Therefore, the arthroprotective effect of THH extract coincided with the increased abundances of beneficial bacteria (immunomodulators and inflammatory suppressors) and the decreased contents of harmful bacteria (inflammatory inducers and LPS producers) in AIA mice.

In addition to affecting the structure of gut microbiota community, THH extract also exerted regulatory effect on the metabolic activities of the intestinal bacteria in AIA mice through PICRUSt analysis. Among these altered metabolic pathways, bacterial lipopolysaccharide biosynthesis was significantly upregulated in AIA mice, but decreased after THH extract treatment. Considering that LPS has adjuvant activity to enhance the production of anti-collagen antibodies involved in the pathogenesis of rheumatoid arthritis [65], such increased synthesis of bacterial LPS may promote TLR-activated inflammatory responses in hosts. Among the regulated metabolic pathways, the saccharide metabolisms including pentose phosphate pathway and galactose metabolism were highly associated with the production of SCFAs [66]. The results imply that THH extract can influence the development of RA by regulating the metabolic pathways of the intestinal flora in AIA mice.

The current therapeutic drugs for RA treatment, including conventional synthetic disease-modifying antirheumatic drugs (DMARDs), targeted synthetic DMARDs, biological DMARDs, and glucocorticoids (GCs), primarily suppress the immune system. Such immunosuppression inevitably increases the risk of infection and malignancy, and the autoimmune response can recur or become more severe once these drugs are abolished. In addition, a large proportion of patients with RA remain under-responsive to these drugs, for example 30% for methotrexate and 37% for biologics [67, 68]. In previous studies, triptolide was validated to accelerate the recovery of gut microbiota balance in ulcerative mice [69]. Tripterine reduced the body weight of obese rats by improving the gut flora structure [70]. The regulatory effect of THH extract on gut microbiota in AIA mice may attribute to the synergistic reactions of active components. Hence, the interaction between the individual components of THH extract and the gut microbiota in the pathogenesis of RA is worthy to be studied in future work. In addition, the specific contribution of each strain of altered bacteria should be further investigated in our following research.

Conclusions

This study demonstrates that THH extract improves CFA-induced AIA in mice, as indicated by alleviated severity of swollen ankle and paw joint, suppressed exudation of the joint cavity, and ameliorated destruction of the articular cartilage. Also, THH extract improves dysbiosis of the gut by decreasing the contents of pathogenic bacteria, such as *Marvinbryantia*, *Desulfovibrio*, *Parabacteroides*, *Bacteroides* and *Butyricimonas*, and increasing the abundances of beneficial bacteria, such as *Bifidobacterium*, *Akkermansia*, *Lactobacillus*, and *Roseburia*. Furthermore, the essential role of the gut microbiota is validated in THH extract-initiated suppressive effect and in the regulation of the TLR4/MyD88/MAPK signaling pathways. In summary, THH extract displayed a high potential in the clinical treatment of RA as a microbial regulator.

Data Availability Statement

The data presented in the study are deposited in the Sequence Read Archive (SRA) 417 database of NCBI repository, accession number PRJNA787415.

References

[1] Croia C, Bursi R, Sutera D, *et al*. One year in review 2019: pathogenesis of rheumatoid arthritis [J]. *Clin Exp Rheumatol*, 2019, **37**(3): 347-357.

[2] Neumann E, Frommer K, Diller M, *et al*. Rheumatoid arthritis [J]. *Z Rheumatol*, 2018, **77**(9): 769-775.

[3] Cross M, Smith E, Hoy D, *et al*. The global burden of rheumatoid arthritis: estimates from the global burden of disease 2010

study [J]. *Ann Rheum Dis*, 2014, **73**(7): 1316-1322.
[4] Smolen JS, Aletaha D, Barton A, *et al*. Rheumatoid arthritis [J]. *Nat Rev Dis Primers*, 2018, **4**: 18001.
[5] Quigley EM. Gut bacteria in health and disease [J]. *Gastroenterol Hepatol (NY)*, 2013, **9**(9): 560-569.
[6] Scher JU, Sczesnak A, Longman RS, *et al*. Expansion of intestinal *Prevotella copri* correlates with enhanced susceptibility to arthritis [J]. *Elife*, 2013, **2**: e01202.
[7] Vaahtovuo J, Munukka E, Korkeamäki M, *et al*. Fecal microbiota in early rheumatoid arthritis [J]. *J Rheumatol*, 2008, **35**(8): 1500-1505.
[8] Johansson K, Askling J, Alfredsson L, *et al*. Mediterranean diet and risk of rheumatoid arthritis: a population-based case-control study [J]. *Arthritis Res Ther*, 2018, **20**(1): 175.
[9] Zeng J, Peng L, Zheng W, *et al*. Fecal microbiota transplantation for rheumatoid arthritis: a case report [J]. *Clin Case Rep*, 2020, **9**(2): 906-909.
[10] Buffie CG, Pamer EG. Microbiota-mediated colonization resistance against intestinal pathogens [J]. *Nat Rev Immunol*, 2013, **13**(11): 790-801.
[11] Akira S, Uematsu S, Takeuchi O. Pathogen recognition and innate immunity [J]. *Cell*, 2006, **124**(4): 783-801.
[12] Guo Y, Wang Y, Shi X, *et al*. A metabolomics study on the immunosuppressive effect of *Tripterygium hypoglaucum* (Levl.) Hutch in mice: the discovery of pathway differences in serum metabolites [J]. *Clin Chim Acta*, 2018, **483**: 94-103.
[13] Zhou X, Liu Q, Zhou X, *et al*. THH relieves CIA inflammation by reducing inflammatory-related cytokines [J]. *Cell Biochem Biophys*, 2020, **78**(3): 367-374.
[14] Guo YL, Gao F, Dong TW, *et al*. Meta-analysis of clinical efficacy and safety of *Tripterygium wilfordii* Polyglycosides Tablets in the treatment of chronic kidney sisease [J]. *Evid-Based Compl Alt*, 2021, **2021**: 6640594.
[15] Segata N, Izard J, Waldron L, *et al*. Metagenomic biomarker discovery and explanation [J]. *Genome Biol*, 2011, **12**(6): R60.
[16] Langille MG, Zaneveld J, Caporaso JG, *et al*. Predictive functional profiling of microbial communities using 16S rRNA marker gene sequences [J]. *Nat Biotechnol*, 2013, **31**(9): 814-821.
[17] Sujitha S, Rasool M. MicroRNAs and bioactive compounds on TLR/MAPK signaling in rheumatoid arthritis [J]. *Clin Chim Acta*, 2017, **473**: 106-115.
[18] Wu X, He B, Liu J, *et al*. Molecular insight into gut microbiota and rheumatoid arthritis [J]. *Int J Mol Sci*, 2016, **17**(3): 431.
[19] Tang W, Zuo JP. Immunosuppressant discovery from *Tripterygium wilfordii* Hook f: the novel triptolide analog (5*R*)-5-hydroxytriptolide (LLDT-8) [J]. *Acta Pharmacol Sin*, 2012, **33**(9): 1112-1118.
[20] Pang J, Ma S, Xu X, *et al*. Effects of rhizome of *Atractylodes koreana* (Nakai) Kitam on intestinal flora and metabolites in rats with rheumatoid arthritis [J]. *J Ethnopharmacol*, 2021, **281**: 114026.
[21] Long C, Yang Y, Wang Y, *et al*. Role of Glutamine-Glutamate/GABA cycle and potential target GLUD2 in alleviation of rheumatoid arthritis by *Tripterygium hypoglaucum* (levl.) Hutch based on metabolomics and molecular pharmacology [J]. *J Ethnopharmacol*, 2021, **281**: 114561.
[22] Jiang Y, Zhong M, Long F, *et al*. Deciphering the active ingredients and molecular mechanisms of *Tripterygium hypoglaucum* (Levl.) Hutch against rheumatoid arthritis based on network pharmacology [J]. *Evid-Based Compl Alt*, 2020, **2020**: 2361865.
[23] Fan D, Guo Q, Shen J, *et al*. The effect of triptolide in rheumatoid arthritis: from basic research towards clinical translation [J]. *Int J Mol Sci*, 2018, **19**(2): 376.
[24] Jiang X, Huang XC, Ao L, *et al*. Total alkaloids of *Tripterygium hypoglaucum* (levl.) Hutch inhibits tumor growth both *in vitro* and *in vivo* [J]. *J Ethnopharmacol*, 2014, **151**(1): 292-298.
[25] Wu W, Cheng R, Boucetta H, *et al*. Differences in multicomponent pharmacokinetics, tissue distribution, and excretion of *Tripterygium* Glycosides Tablets in normal and adriamycin-induced nephrotic syndrome rat models and correlations with efficacy and hepatotoxicity [J]. *Front Pharmacol*, 2022, **13**: 910923.
[26] Kargutkar S, Brijesh S. Anti-rheumatic activity of *Ananas comosus* fruit peel extract in a complete Freund's adjuvant rat model [J]. *Pharm Biol*, 2016, **54**(11): 2616-2622.
[27] Borbély É, Kiss T, Szabadfi K, *et al*. Complex role of capsaicin-sensitive afferents in the collagen antibody-induced autoimmune arthritis of the mouse [J]. *Sci Rep*, 2018, **8**(1): 15916.
[28] Zhang Y, Wang S, Song S, *et al*. Ginsenoside Rg3 alleviates complete Freund's adjuvant-induced rheumatoid arthritis in mice by regulating $CD4^+CD25^+Foxp3^+$Treg Cells [J]. *J Agric Food Chem*, 2020, **68**(17): 4893-4902.
[29] Buch MH, Eyre S, McGonagle D. Persistent inflammatory and non-inflammatory mechanisms in refractory rheumatoid arthritis [J]. *Nat Rev Rheumatol*, 2021, **17**(1): 17-33.
[30] Steinz MM, Santos-Alves E, Lanner JT. Skeletal muscle redox signaling in rheumatoid arthritis [J]. *Clin Sci (Lond)*, 2020, **134**(21): 2835-2850.
[31] Xing L, Schwarz EM, Boyce BF. Osteoclast precursors, RANKL/RANK, and immunology [J]. *Immunol Rev*, 2005, **208**: 19-29.
[32] Wernhoff P, Olofsson P, Holmdahl R. The genetic control of rheumatoid factor production in a rat model of rheumatoid arthritis [J]. *Arthritis Rheum*, 2003, **48**(12): 3584-3596.
[33] Sacre SM, Andreakos E, Kiriakidis S, *et al*. The Toll-like receptor adaptor proteins MyD88 and Mal/TIRAP contribute to the inflammatory and destructive processes in a human model of rheumatoid arthritis [J]. *Am J Pathol*, 2007, **170**(2): 518-525.
[34] Abdollahi-Roodsaz S, Joosten LA, Koenders MI, *et al*. Local interleukin-1-driven joint pathology is dependent on toll-like receptor 4 activation [J]. *Am J Pathol*, 2009, **175**(5): 2004-2013.
[35] Lee EK, Kang SM, Paik DJ, *et al*. Essential roles of Toll-like receptor-4 signaling in arthritis induced by type II collagen antibody and LPS [J]. *Int Immunol*, 2005, **17**(3): 325-333.
[36] He P, Hu Y, Huang C, *et al*. *n*-Butanol extract of *Gastrodia elata* suppresses inflammatory responses in lipopolysaccharide-stimulated macrophages and complete Freund's adjuvant-(CFA-) induced arthritis rats *via* inhibition of MAPK signaling pathway [J]. *Evid-Based Compl Alt*, 2020, **2020**: 1658618.
[37] Premkumar V, Dey M, Dorn R, *et al*. MyD88-dependent and independent pathways of Toll-like receptors are engaged in biological activity of triptolide in ligand-stimulated macrophages [J]. *BMC Chem Biol*, 2010, **10**: 3.
[38] Konig MF. The microbiome in autoimmune rheumatic disease [J]. *Best Pract Res Clin Rheumatol*, 2020, **34**(1): 101473.
[39] Picchianti-Diamanti A, Panebianco C, Salemi S, *et al*. Analysis of gut microbiota in rheumatoid arthritis patients: disease-related dysbiosis and modifications induced by etanercept [J]. *Int J Mol Sci*, 2018, **19**(10): 2938.
[40] Romero-Figueroa MDS, Ramírez-Durán N, Montiel-Jarquín AJ, *et al*. Gut-joint axis: gut dysbiosis can contribute to the onset of rheumatoid arthritis *via* multiple pathways [J]. *Front Cell Infect Microbiol*, 2023, **13**: 1092118.
[41] Attur M, Scher JU, Abramson SB, *et al*. Role of intestinal dysbiosis and nutrition in rheumatoid arthritis [J]. *Cells*, 2022, **11**(15): 2436.

[42] Sun C, Luo Y, Tong H, *et al*. Usefulness of tocilizumab for treating rheumatoid arthritis with myelodysplastic syndrome: a case report and literature review [J]. *Medicine (Baltimore)*, 2018, **97**(25): e11179.
[43] Jubair WK, Hendrickson JD, Severs EL, *et al*. Modulation of inflammatory arthritis in mice by gut microbiota through mucosal inflammation and autoantibody generation [J]. *Arthritis Rheumatol*, 2018, **70**(8): 1220-1233.
[44] Shen X, Miao J, Wan Q, *et al*. Possible correlation between gut microbiota and immunity among healthy middle-aged and elderly people in southwest China [J]. *Gut Pathog*, 2018, **10**: 4.
[45] Biagi E, Nylund L, Candela M, *et al*. Through ageing, and beyond: gut microbiota and inflammatory status in seniors and centenarians [J]. *PLoS One*, 2010, **5**(5): e10667.
[46] Wang Y, Xie Q, Sun S, *et al*. Probiotics-fermented Massa Medicata Fermentata ameliorates weaning stress in piglets related to improving intestinal homeostasis [J]. *Appl Microbiol Biotechnol*, 2018, **102**(24): 10713-10727.
[47] Xiao M, Fu X, Ni Y, *et al*. Protective effects of *Paederia scandens* extract on rheumatoid arthritis mouse model by modulating gut microbiota [J]. *J Ethnopharmacol*, 2018, **226**: 97-104.
[48] Wu XM, Tan RX. Interaction between gut microbiota and ethnomedicine constituents [J]. *Nat Prod Rep*, 2019, **36**(5): 788-809.
[49] Cannarella LAT, Mari NL, Alcântara CC, *et al*. Mixture of probiotics reduces inflammatory biomarkers and improves the oxidative/nitrosative profile in people with rheumatoid arthritis [J]. *Nutrition*, 2021, **89**: 111282.
[50] Li Y, Yang S, Lun J, *et al*. Inhibitory effects of the *Lactobacillus rhamnosus* GG effector protein HM0539 on inflammatory response through the TLR4/MyD88/NF-κB axis [J]. *Front Immunol*, 2020, **11**: 551449.
[51] Schott EM, Farnsworth CW, Grier A, *et al*. Targeting the gut microbiome to treat the osteoarthritis of obesity [J]. *JCI Insight*, 2018, **3**(8): e95997.
[52] Kwon Y, Park C, Lee J, *et al*. Regulation of bone cell differentiation and activation by microbe-associated molecular patterns [J]. *Int J Mol Sci*, 2021, **22**(11): 5805.
[53] Tamanai-Shacoori Z, Smida I, Bousarghin L, *et al*. *Roseburia* spp. : a marker of health? [J]. *Future Microbiol*, 2017, **12**: 157-170.
[54] Liu Z, Wu Y, Luo Y, *et al*. Self-balance of intestinal flora in spouses of patients with rheumatoid arthritis [J]. *Front Med (Lausanne)*, 2020, **7**: 538.
[55] Volkova A, Ruggles KV. Predictive metagenomic analysis of autoimmune disease identifies robust autoimmunity and disease specific microbial signatures [J]. *Front Microbiol*, 2021, **12**: 621310.
[56] Sun Y, Chen Q, Lin P, *et al*. Characteristics of gut microbiota in patients with rheumatoid arthritis in Shanghai, China [J]. *Front Cell Infect Microbiol*, 2019, **9**: 369.
[57] Hong CJ, Chen SY, Hsu YH, *et al*. Protective effect of fermented okara on the regulation of inflammation, the gut microbiota, and SCFAs production in rats with TNBS-induced colitis [J]. *Food Res Int*, 2022, **157**: 111390.
[58] Dürholz K, Hofmann J, Iljazovic A, *et al*. Dietary short-term fiber interventions in arthritis patients increase systemic SCFA levels and regulate inflammation [J]. *Nutrients*, 2020, **12**(10): 3207.
[59] Van de Wiele T, Van Praet JT, Marzorati M, *et al*. How the microbiota shapes rheumatic diseases [J]. *Nat Rev Rheumatol*, 2016, **12**(7): 398-411.
[60] Ivanov II, Atarashi K, Manel N, *et al*. Induction of intestinal Th17 cells by segmented filamentous bacteria [J]. *Cell*, 2009, **139**(3): 485-498.
[61] Maeda Y, Kurakawa T, Umemoto E, *et al*. Dysbiosis contributes to arthritis development *via* activation of autoreactive T cells in the intestine [J]. *Arthritis Rheumatol*, 2016, **68**(11): 2646-2661.
[62] Kohashi O, Kuwata J, Umehara K, *et al*. Susceptibility to adjuvant-induced arthritis among germfree, specific-pathogen-free, and conventional rats [J]. *Infect Immun*, 1979, **26**(3): 791-794.
[63] Tlaskalová-Hogenová H, Stepánková R, Hudcovic T, *et al*. Commensal bacteria (normal microflora), mucosal immunity and chronic inflammatory and autoimmune diseases [J]. *Immunol Lett*, 2004, **93**(2-3): 97-108.
[64] Xu H, Pan LB, Yu H, *et al*. Gut microbiota-derived metabolites in inflammatory diseases based on targeted metabolomics [J]. *Front Pharmacol*, 2022, **13**: 919181.
[65] Kasperkiewicz K, Świerzko AS, Przybyła M, *et al*. The Role of *Yersinia enterocolitica* O: 3 lipopolysaccharide in collagen-induced arthritis [J]. *J Immunol Res*, 2020, **2020**: 7439506.
[66] Macfarlane S, Macfarlane GT. Regulation of short-chain fatty acid production [J]. *Proc Nutr Soc*, 2003, **62**(1): 67-72.
[67] Szostak B, Machaj F, Rosik J, *et al*. Using pharmacogenetics to predict methotrexate response in rheumatoid arthritis patients [J]. *Expert Opin Drug Metab Toxicol*, 2020, **16**(7): 617-626.
[68] Moulis G, Pugnet G, Costedoat-Chalumeau N, *et al*. Efficacy and safety of biologics in relapsing polychondritis: a French national multicentre study [J]. *Ann Rheum Dis*, 2018, **77**(8): 1172-1178.
[69] Wu H, Rao Q, Ma GC, *et al*. Effect of triptolide on dextran sodium sulfate-induced ulcerative colitis and gut microbiota in mice [J]. *Front Pharmacol*, 2020, **10**: 1652.
[70] Hu W, Wang L, Du G, *et al*. Effects of microbiota on the treatment of obesity with the natural product celastrol in rats [J]. *Diabetes Metab J*, 2020, **44**(5): 747-763.

Cite this article as: HU Jianghui, NI Jimin, ZHENG Junping, GUO Yanlei, YANG Yong, YE Cheng, SUN Xiongjie, XIA Hui, LIU Yanju, LIU Hongtao. *Tripterygium hypoglaucum* extract ameliorates adjuvant-induced arthritis in mice through the gut microbiota [J]. *Chin J Nat Med*, 2023, **21**(10): 730-744.